Available online at www.sciencedirect.com
SCIENCE DIRECT®
Journal of Magnetic Resonance 174 (2005) 152–162
JMR Journal of Magnetic Resonance
www.elsevier.com/locate/jmr

Periodicity, planarity, residual dipolar coupling, and structures

Joseph D. Walsh, Yun-Xing Wang *

Protein Nucleic Acid Interaction Section, Structural Biophysics Laboratory, NCI-Frederick, NIH, Frederick, MD 21702, USA

Received 22 October 2004; revised 30 December 2004

Abstract

The periodic behavior of residual dipolar couplings (RDCs) arising from nucleic acid and protein secondary structures is shown to be more complex and information-rich than previously believed. We have developed a theoretical framework which allows the bond vector orientation of nucleic acids and the peptide plane orientations of protein secondary structures to be extracted from their Dipolar waves. In this article, we focus on utilizing ''Dipolar waves'' of peptides to extract structure information, and describe in more detail the fundamental principles of the relationship between the periodicities in structure and RDCs, the practical procedure to extract peptide plane orientation information from RDC data, and assessment of errors using Monte-Carlo simulations. We demonstrate the utility of our method for two model α-helices, one kinked and one curved, and as well as an irregular β-strand. Published by Elsevier Inc.

Keywords: RDC; Periodicity; Planarity; Secondary structure

1. Introduction

The vast majority of protein and nucleic acid structures consist of highly regular secondary structures, such as α-helices, β-strands, and duplexes. These regular secondary structures are the building blocks that are arranged in three-dimensional space to form the scaffolds of protein and nucleic acid structures. These building blocks are highly repetitive and periodical in nature, a property which is reflected in any type of geometric physical measurements, such as residual dipolar couplings (RDCs) [1–3].

When a protein or nucleic acid sample is dissolved in an alignment medium (pf1 phage, DMPC/DHPC, purple membrane, etc.), dipolar interactions between spins are no longer averaged to zero. In a weakly aligned solution, this interaction is called the residual dipolar coupling because it is only a factor of 10^{-3} compared to its static value [4]. The amplitude and sign of the RDC depends on the orientation of the vector connecting the pair of spins relative to the alignment axis system in a magnetic field. For this reason, the RDC is said to contain orientation information about how a pair of spins (atoms) are aligned in relation to a common reference system, i.e., the alignment tensor axis system, and have been used for structure determination in various ways since the late 1990s [5–8].

Since the RDC reflects the orientations of a spin pair, it is rather intuitive and obvious in retrospect that the repetitiveness and periodicity in regular protein and nucleic acid secondary structures are closely correlated to the amplitude and sign of the RDC. When they are plotted vs. the residue number of a regular secondary structure, the RDCs show a periodical pattern (Fig. 1) [1–3]. The significance of this Dipolar wave should not be underestimated. First, it provides a direct link between regular secondary structure and RDC measurements, as illustrated in Fig. 1. What is shown in Fig. 1 is not only the periodic pattern of the Dipolar wave but also a certain resemblance of the Dipolar wave to the structure itself if the molecule is aligned at particular angles relative to the alignment tensor axis system. In other words, the wave itself is indicative of the type of second-

* Corresponding author. Fax: +1 301 846 6231.
E-mail address: wangyu@ncifcrf.gov (Y.-X. Wang).

1090-7807/$ - see front matter. Published by Elsevier Inc.
doi:10.1016/j.jmr.2005.01.018

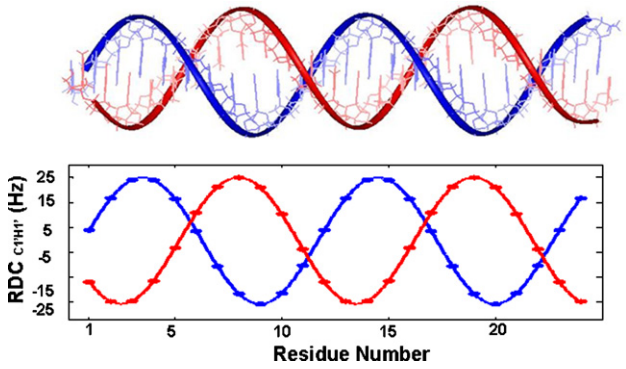

Fig. 1. The periodicity inherent in a duplex structure is strikingly mirrored in the Dipolar Waves when a duplex is orientated at a particular angle. In this case, the Dipolar wave from the ribose C1′H1′ for a B-form DNA duplex oriented at $(\Theta, \Phi) = (40°, 90°)$ is shown.

ary structure element. Second, the shape and amplitude of the Dipolar waves depend on the orientation of the structure elements in relation to the alignment axis system [2]. When the RDC is explicitly written in terms of the spin pair orientation in a molecular frame in relationship to the alignment tensor system, one can extract the orientation information of spin pairs as well as that of the secondary structure elements [2].

In the case of protein, the peptide backbone consists of consecutive peptide planes. Within a peptide plane, there are a number of spin pairs whose RDCs are experimentally measurable. The orientation of inter-nuclear vectors connecting these spin pairs within the plane is dictated by the constraints of planarity of the peptide backbone and its chemical bond angles. When the orientations of inter-nuclear vectors within the plane are considered collectively, the RDC can be expressed explicitly in terms of the plane orientation (Eq. (4)). The plane orientation is defined by its normal vector, plus a rotation around the normal (Fig. 3) in spherical coordinates. The significance of the interpretation of the RDC in terms of the planarity as the intrinsic peptide backbone structural feature is twofold. First, it eliminates numerous possible bond vector orientations that would otherwise satisfy RDC values when RDCs are considered individually but significantly deviate either from planarity or the chemical bond angles of the peptide plane. Second, when considering the peptide plane normal vectors these normals also exhibit periodicity in regular secondary structure. Therefore, when the RDC is expressed in terms of both planarity and periodicity in an explicit analytical equation (Eq. (4)), RDCs can be interpreted more directly in a "structural" way.

Using Eq. (4) one can extract orientation information pertinent to both individual bond vectors and secondary structure elements because the structure is determined directly in the alignment tensor axis system using the intrinsic constraints of periodicity and planarity (unpublished result). This report gives a more detailed account of the intricate relation between the RDC and periodicity and planarity, and how this can be used to derive local structural information of individual peptide plane orientations in a global reference system. This approach is distinct from the existing singular value decomposition (SVD) method [7] that relates the alignment tensor to a known molecular structure (solving for the Saupe matrix elements) without yielding new local structure information. We should point out that relating bond vectors within a peptide plane to solid state NMR measurements has been considered previously [9–11]. In this report we present a detailed account for a rigorous theoretical treatment of the correlation between the periodicity, planarity, and RDC measurement.

2. Theory

2.1. Periodicity in the RDC

For structural elements of a known type, such as the duplex in nucleic acids, or a protein α-helix or β-strand, the RDC between nuclei A and B, D_{AB}, can be expressed in terms of the coordinate system most natural to the structure. In this coordinate system, the orientation of the secondary structure mean axis is defined by the spherical angles (Θ, Φ) with respect to the alignment frame, and an individual inter-nuclear vector is referenced to this axis by use of spherical angles (δ_i, ρ_i). The slant angle, δ_i is the angle the inter-nuclear vector AB makes with the structure axis, with ρ_i the phase of the inter-nuclear vector about this axis. For a structural element with axis oriented along the principle alignment axis Z, the inter-nuclear vector AB is hence given in the usual spherical coordinate notation as

$$\hat{r}^{\mathrm{AB,sec.str.}} = (\sin\delta^{\mathrm{AB}}\cos\rho^{\mathrm{AB}}, \sin\delta^{\mathrm{AB}}\sin\rho^{\mathrm{AB}}, \cos\delta^{\mathrm{AB}}) \quad (1)$$

with the inter-nuclear vector orientation for an arbitrary alignment (Θ, Φ) given by $\hat{r}^{\mathrm{AB}} = R_z(\Phi)R_y(\Theta)\hat{r}^{\mathrm{AB,sec.str.}}$.

By expressing the RDC equation using this coordinate system, RDCs are seen to possess periodicity in the azimuthal angle, ρ_i whose amplitude is modulated by coefficients dependent on Θ, Φ, and δ_i [2]

$$\begin{aligned} D_{\mathrm{AB},i} = {} & C_1(\Theta,\Phi,\delta_i)\cos 2\rho_i + C_2(\Theta,\Phi,\delta_i)\sin 2\rho_i \\ & + C_3(\Theta,\Phi,\delta_i)\cos\rho_i + C_4(\Theta,\Phi,\delta_i)\sin\rho_i \\ & + C_5(\Theta,\Phi,\delta_i). \end{aligned} \quad (2)$$

This equation is universally applicable to any periodical structural element. In it, $\rho_i = \rho_1 + 2\pi(i-1)/T$ is the phase of the inter-nuclear vector AB in the ith residue, which is related to the phase of the inter-nuclear vector of the first residue, ρ_1, and to the period, T ($T \approx 11$ residues/turn for A-form $T \approx 10$ residues/turn for B-form nucleic acids, and $T \approx 3.6$ residues/turn for an α-helix and $T \approx 2$ residues/turn for a β-strand in a protein). The coefficients $C_k = C_k(\Theta, \Phi, \delta_i)$ are given in Table 1.

Table 1
RDC-periodicity Eq. (2) coefficients

$C_1(\Theta,\Phi,\delta_i) = (3D_a/16)(4 + 6R\cos 2\Phi + R\cos 2(\Phi - \Theta) - 4\cos 2\Theta + R\cos 2(\Phi + \Theta))\sin^2\delta_i$
$C_2(\Theta,\Phi,\delta_i) = (-3D_a/2)R\cos\Theta\ \sin 2\Phi\sin^2\delta_i$
$C_3(\Theta,\Phi,\delta_i) = (3D_a/4)(R\cos 2\Phi - 2)\sin 2\Theta\sin 2\delta_i$
$C_4(\Theta,\Phi,\delta_i) = -6D_aR\sin\Theta\sin\Phi\cos\Phi\sin\delta_i\cos\delta_i$
$C_5(\Theta,\Phi,\delta_i) = (D_a/32)(4 + 6R\cos 2\Phi - 3R\cos 2(\Phi - \Theta) + 12\cos 2\Theta - 3R\cos 2(\Phi + \Theta))(3\cos 2\delta_i + 1)$

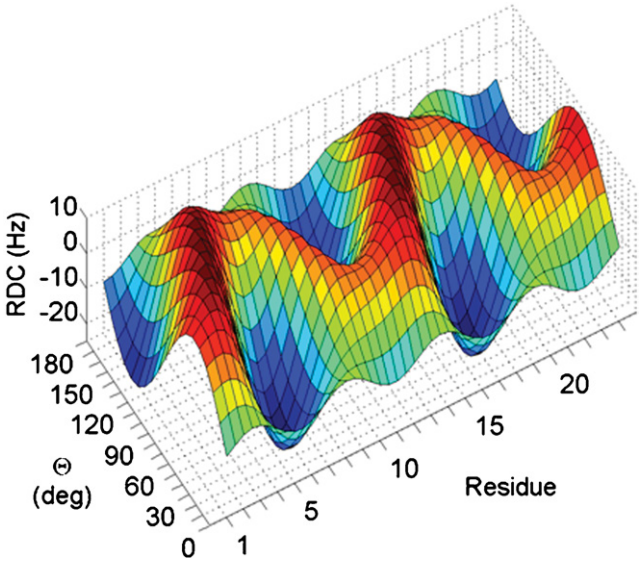

Fig. 2. A three-dimensional view of the dependence of the shape of an Dipolar wave on the orientation of the secondary structure polar angle Θ. Shown is the simulated Dipolar wave (Eq. (2)) arising from the C1′H1′ of a 24-mer of A-RNA as a continuous function of the duplex axis polar angle Θ. The azimuthal angle is fixed at $\Phi = 20°$, with $D_a = -14.5$ and $R = 1/3$.

The periodicity in ρ_i in Eq. (2) reveals a pronounced dependence of the shape and amplitude of the Dipolar wave on Θ and Φ, and therefore bears information about the alignment of a structure in an alignment media. Hence, the equation can be used to extract orientation parameters from a Dipolar wave. The complex shapes of Dipolar waves and their dependence on the alignment polar angle Θ is illustrated in a three-dimensional plot in Fig. 2. Eq. (2) shows analogous functional dependence of the Dipolar wave shape with Φ (not shown). We note that for an inter-nuclear vector such as the NH vector with slant angle lying close to the secondary structure element axis (small δ_i), the dipolar wave (Eq. (2)) may appear sinusoidal. However, this approximate sinusoidal behavior is not maintained for all orientations of the secondary structure axis in the alignment frame.

2.2. RDC and peptide plane periodicity

Although the principle of periodicity discussed in the previous sections is applicable to any periodic structural elements, in the case of regular protein secondary structures, the sampling rate of the Dipolar wave for each type of spin pair is approximately 3.6 and 2 residues/turn for α-helix and β-strand, respectively, far fewer than that of the nucleic acid duplex. Consequently, the Dipolar wave is in general not well-enough defined to extract useful orientation information if individual types of spin pairs are considered separately. However, peptide backbone atoms lie within consecutive peptide planes. Therefore, the geometric relationships among spin pairs in a peptide plane and the planarity constraint of the peptide linkage can be utilized so that several types of RDCs can be considered collectively to orient the common unit of the peptide plane. This is done by building the geometric relationships of the peptide plane into the RDC equation, thereby expressing the RDCs in terms of the plane orientation. The orientation of the peptide plane is defined by three angles as shown in Fig. 3. The first two of these angles are the tilt, δ^n, and phase, ρ^n, which define the normal vector of the peptide plane according to $\hat{n} = (\sin\delta^n\cos\rho^n, \sin\delta^n\sin\rho^n, \cos\delta^n)$. The third angle is γ^{AB}, which represents the rotational orientation of the AB inter-nuclear vector in the plane about the normal vector. We refer to γ^{AB} as the pitch, because in the case of the α-helix, γ^{AB} is a measure of the pitch of the helix at that plane position.

Using these three angles, any inter-nuclear vector in the jth peptide plane in a structural element with its axis on the alignment frame principle axis Z can be written as (for clarity we have omitted the peptide plane subscript j from the angles δ^n, ρ^n, and γ^{AB})

$$\hat{r}_j^{AB,\text{sec .str.}} = \begin{pmatrix} -\cos\delta^n\cos\rho^n\cos\gamma^{AB} - \sin\rho^n\sin\gamma^{AB} \\ -\cos\delta^n\sin\rho^n\cos\gamma^{AB} + \cos\rho^n\sin\gamma^{AB} \\ \sin\delta^n\cos\gamma^{AB} \end{pmatrix}. \tag{3}$$

Using Eq. (3), we can now obtain the expression for an inter-nuclear vector in any structural element aligned at an arbitrary orientation (Θ,Φ) by two rotations: $\hat{r}_j^{AB} = R_z(\Phi)R_y(\Theta)\hat{r}^{AB,\text{sec .str.}}$.

To define the pitch angle of the peptide plane, one of the in-plane inter-nuclear vectors was used to serve as a reference. We arbitrarily defined the peptide plane pitch angle γ^n as the pitch angle of the $\hat{r}_j^{HN}$ inter-nuclear vector. This means that the value of the pitch angle of any other inter-nuclear vector $\hat{r}_j^{AB}$ will be related to that of $\hat{r}_j^{HN}$ by $\gamma^{AB} = \gamma^n + \text{const.}$, where const. $= 56.5°$, $-60.5°$, and $-37.4°$ for $\hat{r}_j^{C\alpha C}$, $\hat{r}_j^{NC'}$, and $\hat{r}_j^{HC'}$, respectively.

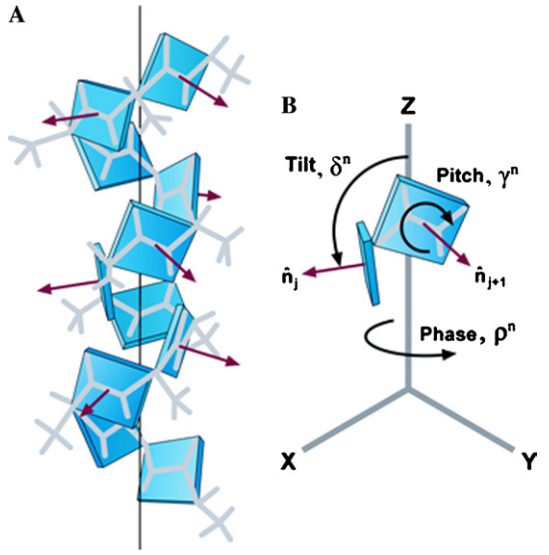

Fig. 3. (A) An α-helix backbone structure defined by consecutive peptide plane orientations. The plane normal vectors which define the plane orientations are indicated with red arrows. (B) The definition of the peptide plane orientation tilt (δ^n), phase (ρ^n), and pitch (γ^n). The orientation of the peptide plane normal vector $\hat{n}$ is determined by the tilt and phase in the usual spherical coordinate sense according to $\hat{n} = (\sin\delta^n \cos\rho^n, \sin\delta^n \sin\rho^n, \cos\delta^n)$. The pitch is the clockwise rotation of an inter-nuclear vector about the normal vector.

These angles represent the mean value from the helices of the high resolution crystal structure of subtilisin [12]. Therefore, a peptide plane orientation is uniquely determined by the angles $(\delta^n, \rho^n, \gamma^n)$, with the actual RDC values obtained from these angles plus the constant angular offset of the particular spin pair AB in question.

This means that the RDC equation can be written as a function of the three peptide plane orientation angles

$$\begin{aligned} D_j^{\mathrm{AB}}(\Theta,\Phi,\delta^n,\rho^n,\gamma^n) &= \mathrm{Da}\{(-1+3R/2)[\sin\Phi(\cos\delta^n\sin\rho^n\cos\gamma^{\mathrm{AB}} - \cos\rho^n\sin\gamma^{\mathrm{AB}}) \\ &\quad - \cos\Theta\cos\Phi(\cos\delta^n\cos\rho^n\cos\gamma^{\mathrm{AB}} + \sin\rho^n\sin\gamma^{\mathrm{AB}}) \\ &\quad + \sin\Theta\cos\Phi\sin\delta^n\cos\gamma^{\mathrm{AB}}]^2 - (1+3R/2) \\ &\quad \times [-\cos\Phi(\cos\delta^n\sin\rho^n\cos\gamma^{\mathrm{AB}} - \cos\rho^n\sin\gamma^{\mathrm{AB}}) \\ &\quad - \cos\Theta\sin\Phi(\cos\delta^n\cos\rho^n\cos\gamma^{\mathrm{AB}} + \sin\rho^n\sin\gamma^{\mathrm{AB}}) \\ &\quad + \sin\Theta\sin\Phi\sin\delta^n\cos\gamma^{\mathrm{AB}}]^2 + 2[\cos\Theta\sin\delta^n\cos\gamma^{\mathrm{AB}} \\ &\quad + \sin\Theta(\cos\delta^n\cos\rho^n\cos\gamma^{\mathrm{AB}} + \sin\rho^n\sin\gamma^{\mathrm{AB}})]^2\}. \end{aligned} \tag{4}$$

The plane orientation angles can therefore be extracted using the RDCs of multiple in-plane spin pairs AB, all of which must fit a common compliment of $(\delta^n, \rho^n, \gamma^n)$. The determination of the peptide plane orientation is further aided by RDCs from neighboring C_α tetrahedral centers (see below). As a result of this, the Dipolar wave, whose concept has gone beyond a simple wave, is well defined by $N \times 3.6$ points/turn for an α-helix (N is the number of types of RDC that are experimentally measured). There are 4–5 in-plane commonly measured RDCs per peptide plane, plus two additional RDCs involving the C_α tetrahedral center (see C_α tetrahedral center, below).

Since the RDC bears no translational information as far as the relationship between a spin pair and alignment tensor axis is concerned, the spin pairs within the peptide plane can be considered as vectors that fan out in a radial distribution. The relative angles between the vectors are those of the relative bond angles in the peptide plane. Therefore, the RDCs of this collection of spin pairs are also periodic when plotted against their pitch angle in the plane (Fig. 4A). This "peptide plane periodicity" wave is not evenly sampled because of the nature

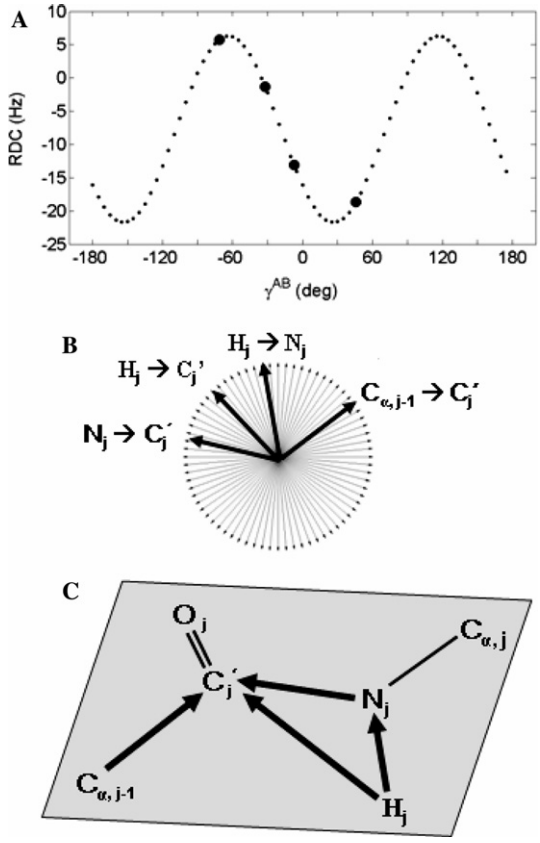

Fig. 4. The peptide plane RDC periodicity. (A) The calculated Dipolar wave (small •) generated by a hypothetical set of spin-pairs in the peptide plane whose inter-nuclear vector pitch angle, γ^{AB}, ranges from −180° to +180°. The RDCs were calculated using the axial alignment of a HN spin-pair, $D_{\mathrm{a}}^{\mathrm{HN}} = -15.0$ and R=2/3 with fixed orientations $(\delta^n, \rho_1^n) = (101.9°, 0°)$ and $(\Theta, \Phi) = (20°, 60°)$ using the Eq. (4). The HN-normalized RDCs corresponding to the measurable ${}^1D_{NH}$, ${}^1D_{C\alpha C'}$, ${}^1D_{NC'}$, and ${}^3D_{HC'}$ are shown lying on the Dipolar wave (large ●). (B) The angular distribution of in-plane peptide bond vectors. The relative angles among the bond vectors are defined by chemical geometry. The background thin arrows are separated by 5°. If RDCs were generated from HN bond vectors at the orientations of the thin arrows, the Dipolar wave shown in (A) would result. (C) The experimentally accessible RDCs are represented by the vectors connecting the spin-pairs from which they arise. The vectors represent an angular sampling range of ~120°, or about 2/3 of the period of a peptide plane Dipolar wave.

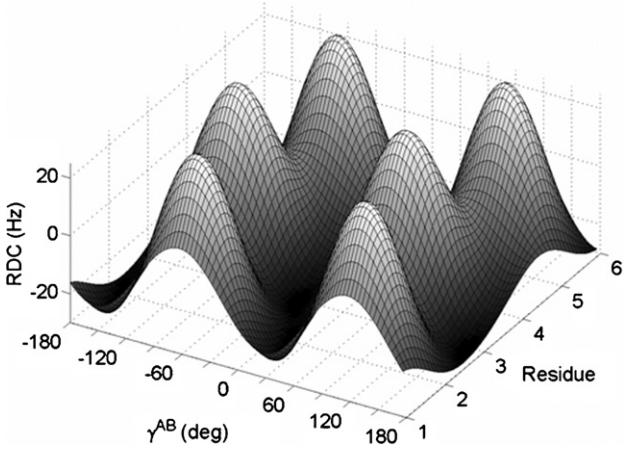

Fig. 5. The expanded Dipolar wave concept incorporates both secondary structure and peptide plane periodicity. The peptide plane periodicity (in pitch, γ) is shown nested within the secondary structure periodicity (in residue number/phase ρ). The RDCs were generated from a model α-helix with $(\delta^n, \rho_1^n) = (101.9°, 0°)$ and $(\Theta, \Phi) = (20°, 60°)$ $D_a^{HN} = -14.5$, $R = 2/3$.

of the peptide plane geometry (Figs. 4B and C). The "peptide plane periodicity" represents a second dimension that the concept of the Dipolar wave has been expanded into. If the RDCs of a protein α-helix are plotted on the z-axis against the "peptide plane periodicity" pitch angle, γ^{AB}, on the x-axis and the peptide plane phase, ρ^n (as represented by the peptide plane number) along the y-axis, the full nature of the expanded Dipolar wave concept becomes apparent (Fig. 5). The entire surface of this expanded Dipolar wave depends on the overall alignment of the secondary structure element as well as the particular orientations of individual plane normal vectors.

2.3. Planarity and C_α tetrahedral center

Like the peptide plane, the tetrahedral configuration around C_α, represents a well-defined chemical geometry in proteins. The RDCs of pairs of nuclei associated with the C_α tetrahedral center place constraints on the relative orientations of the peptide planes that flank it. The geometric relationship between the tetrahedral center and neighboring peptide planes is well conserved in high resolution crystal structure (see Table 2). In particular, the tetrahedral angle $T_{NC\alpha C'}$ between N, C_α, and C′ as well as the relationships between the plane made by $C_\alpha N$, and $C_\alpha C'$ and the $C_\alpha H_\alpha$ and $C_\alpha C_\beta$ inter-nuclear vectors are well conserved. These relationships were exploited to refine peptide plane orientations.

The tetrahedral center and the neighboring two peptide plane orientations $(\delta_j^n, \rho_j^n, \gamma_j^n)$ and $(\delta_{j+1}^n, \rho_{j+1}^n, \gamma_{j+1}^n)$ were correlated to the RDCs associated with C_α. Analytically this was accomplished by first noting that two neighboring plane orientations give rise to the inter-nuclear vectors $\hat{r}_j^{C\alpha N}$ and $\hat{r}_{j+1}^{C\alpha C'}$ (Eq. (3)) and therefore define the tetrahedral angle $T_{NC\alpha C'}$ between them. A plane orientation may therefore be in part determined on the basis of best agreement with the nominal protein tetrahedral angle at C_α (Table 2). Second, neighboring peptide plane orientations give rise to a unique $\hat{r}_j^{C\alpha H\alpha}$ and $\hat{r}_j^{C\alpha C\beta}$ from which a theoretical ${}^1D_{C\alpha H\alpha}$ and ${}^1D_{C\alpha C\beta}$ can be calculated and compared to their experimental values, further refining the plane orientations. To generate $\hat{r}_j^{C\alpha H\alpha}$ and $\hat{r}_j^{C\alpha H\beta}$ from the neighboring peptide planes, the $\hat{r}_j^{C\alpha N}$ and $\hat{r}_{j+1}^{C\alpha C'}$ inter-nuclear vectors were used to construct a local right-handed coordinate system at the tetrahedral center $C_{\alpha,j}$ (the tetrahedral center j and associated inter nuclear vectors $\hat{r}_j^{C\alpha H\alpha}$ and $\hat{r}_j^{C\alpha H\beta}$ are defined to lie between planes j and $j+1$).

$$\begin{aligned} \hat{y}_j &= \hat{r}_j^{C\alpha N}, \\ \hat{x}_j &= (\hat{r}_{j+1}^{C\alpha C'} - \hat{y}_j(\hat{y}_j \cdot \hat{r}_{j+1}^{C\alpha C'}))/\|\hat{r}_{j+1}^{C\alpha C'} - \hat{y}_j(\hat{y}_j \cdot \hat{r}_{j+1}^{C\alpha C'})\|, \\ \hat{z}_j &= \hat{x}_j \times \hat{y}_j. \end{aligned} \tag{5}$$

The $\hat{r}_j^{C\alpha H\alpha}$ and ($\hat{r}_j^{C\alpha C\beta}$ inter-nuclear vectors can then be constructed by rotating the $\hat{z}_j$ vector about the axis $\hat{a}$ by angle κ, and about the axis $\hat{b}$ by angle λ, respectively:

Table 2
Tetrahedral parameters for the C_α center

	Angles (°)					
	$T_{NC\alpha C'}$	$\sigma(T_{NC\alpha C'})$	κ	λ	$\sigma(C_\alpha H_\alpha)$	$\sigma(C_\alpha C_\beta)$
α-helix	111.4	1.32	33.56	141.69	0.94	1.76
β-strand	109.13	2.09	34.05	142.89	1.27	2.03
All other	110.82	2.38	34.06	142.53	1.86	3.20
	Vectors					
	$\hat{a}$	$\hat{b}$				
α-helix	(0.564, −0.826, 0.000)	(0.548, −0.835, 0.000)				
β-strand	(0.579, −0.815, 0.000)	(0.577, −0.816, 0.000)				
All other	(0.568, −0.823, 0.000)	(0.564, −0.823, −0.000)				

Parameters were extracted from the 0.78 Å resolution Subtilisin crystal structure (pdb code 1GCI) [12]. The angular RMSD of the tetrahedral angle C_α makes with backbone atoms is signified by $\sigma(T_{NC\alpha C'})$. The accuracy of the transformation using the parameters $\hat{a}$ and κ of the table is signified by $\sigma(C_\alpha H_\alpha)$, which is the average angular difference between the $\hat{r}^{C\alpha H\alpha}$ inter-nuclear vector calculated from $\hat{a}$ and κ, and the inter-nuclear vector from the crystal structure.

$$\hat{r}_j^{C\alpha H\alpha} = R_{\hat{a}}(\kappa)\hat{z}_j, \tag{6a}$$

$$\hat{r}_j^{C\alpha C\beta} = R_{\hat{b}}(\lambda)\hat{z}_j. \tag{6b}$$

The axes $\hat{a}$ and $\hat{b}$ (expressed in the local coordinate system basis of Eq. (5)) and angles κ and λ are properties of the peptide C_α geometry and are given in Table 2.

3. Methods

3.1. Procedure to extract the plane orientations from RDCs

Periodicity, planarity, and the tetrahedral center are used to extract the peptide plane orientations of a secondary structure through a three-step process outlined below.

3.1.1. Alignment fit

The orientation (Θ, Φ) of a secondary structure element in the alignment frame is determined using all available RDC data related to the peptide backbone. The data were fit using Eqs. (2) and (4) using a common alignment (Θ, Φ). The fit alignment angles (Θ, Φ) were constrained to lie in the first "quadrant" of the sphere, Θ: $[0°, 90°]$, Φ: $[0°, 180°]$, since there are four equivalent orientations of a secondary structure element which yield the same Dipolar wave: $(\Theta, \Phi, \rho_1^n, \rho_1^{C\alpha H\alpha})$, $(\Theta, \Phi + \pi, \rho_1^n, \rho_1^{C\alpha H\alpha})$, $(\pi - \Theta, \pi - \Phi, \rho_1^n + \pi, \rho_1^{C\alpha H\alpha} + \pi)$ $(\pi - \Theta, 2\pi - \Phi, \rho_1^n + \pi, \rho_1^{C\alpha H\alpha} + \pi)$.

The in-plane RDCs were fit under the assumption that the planes in the secondary structure possessed a uniform value for the tilt angle and the pitch angle, denoted as $\bar{\delta}^n$ and $\bar{\gamma}^n$, respectively. The values of the uniform tilt and pitch angles were fit, but required to lie within a range of $\pm 30°$ of the nominal tilt and pitch value for the particular type of secondary structure in question (see Table 3). The phase of the first peptide plane, ρ_1^n, was also fit (in a range 0–2π), with all subsequent phases of planes $j = 1, \ldots, n$ generated from it by $\rho_j^n = \rho_1^n + 2\pi(j-1)/T$. For α-helices the nominal value for the period of $T = 3.6$ residues (planes) per turn was used, and in the case of the β-strand the period was optimized in the range from $T = 1.6$ to 2.4 residues (planes) per turn. For each set of non-plane RDCs, a uniform tilt angle and the initial phase was fit (see Eq. (2) and Table 3).

3.1.2. Peptide plane fit

The determination of the precise orientation of individual peptide planes was accomplished with Eq. (4) utilizing the secondary structure orientation (Θ, Φ) determined in the alignment fit step. The RDCs arising from each peptide plane were fit to Eq. (4) by optimizing the three peptide plane angles ρ^n, δ^n, and γ^n simultaneously. For each plane, each angle was optimized in a limited range about the corresponding value obtained in the alignment fit step: $\bar{\delta}^n \pm 30°$, $\rho_j^n \pm 30° = \rho_1^n + 360°(j-1)/T \pm 30°$, $\bar{\gamma}^n \pm 30°$. This range allowed for peptide plane orientations to be fit which arise from local deviations in structure as well as an overall curvature or kink of the secondary structure (see Section 4). However, for a particular set of in-plane RDCs, there may be more than one corresponding plane orientation. Within the allowed angular fit range for tilt, phase, and pitch there may be up to four separate plane orientations with identical RDCs for in-plane spin-pairs. This ambiguity was resolved and the correct peptide plane orientations determined by use of the relationship between successive peptide planes and the tetrahedral center.

3.1.3. Peptide plane orientations and the tetrahedral center

The backbone secondary structure is completely determined by the sequence of peptide plane orienta-

Table 3
Nominal parameters for secondary structure elements (InsightII)

		Slant angles (δ^{AB})				
	AB:	C1′H1′	C2′H2′	C3′H3′	C4′H4′	Imino
Nucleic acid						
A-form (RNA)		134.7°	72.9°	76.0°	83.2°	106.2° (G)/105.0° (U)
B-Form (DNA)		67.4°	—	−86.4°	123.2°	84.7° (G)/84.0° (T)
	AB:	HN	$C_\alpha C'$	NC′	$C_\alpha H_\alpha$	$C_\alpha C\beta$
Protein						
α-helix		13.8°	46.0°	71.7°	58.0°	149.0°
β-strand		76.0°	36.0°	130.3°	87.4°	91.7°
		Peptide plane angles				
		Tilt (δ^n)	Pitch (γ^n)			
α-helix		101.9°	−7.3°			
β-strand		119.3°	−73.9°			

tions of which it is made up. Because some peptide planes possess multiple possible orientations for a given in-plane RDC data set this results in multiple possible sequences of peptide planes orientations (multiple possible backbone structures). The correct peptide plane sequence (backbone structure) was determined by making use of the tetrahedral centers that flank a peptide plane. For every possible sequence of peptide plane orientations arising from the individual peptide plane fitting step, corresponding tetrahedral ${}^1D_{C\alpha H\alpha}$ and $T_{\mathrm{NC}\alpha\mathrm{C}'}$ values were calculated (see Section 2). The possible sequences of peptide planes were then sorted by the sum of the ${}^1D_{C\alpha H\alpha}$ and $T_{\mathrm{NC}\alpha\mathrm{C}'}$ RMSDs to their target values. The protein backbone structure was taken to be given by the sequence of plane orientations with the lowest RMSD to the target ${}^1D_{C\alpha H\alpha}$ or ${}^1D_{C\alpha H\beta}$ as well as lowest RMSD to the nominal tetrahedral angle $T_{\mathrm{NC}\alpha\mathrm{C}'}$.

3.2. Error estimation

Monte-Carlo simulations were run in order to determine the sensitivity of the determined peptide plane orientations to random error in the RDCs. Normally distributed noise with standard deviation $\sigma = 1.5$ Hz was superimposed on ${}^1D_{C\alpha H\alpha}$ $\sigma = 0.5$ Hz noise superimposed on ${}^1D_{NH}$, and $\sigma = 0.25$ Hz noise was superimposed on ${}^1D_{C'C\alpha}$, and ${}^1D_{C'N}$, with the noise distributions tails cut off at $\pm 2\sigma$. The tilt, phase, and pitch angles obtained from the fit of the four RDC data sets with superimposed noise show a distribution about the tilt, phase, and pitch angles obtained without superimposed noise. The width of this distribution is dependent upon the orientation of the peptide plane in the alignment tensor system (see Section 4).

3.3. Model secondary structures

Two model α-helices and a β-strand were constructed using the Biopolymer module of InsightII (Accelrys, San Diego, CA). The first helix was significantly kinked, consisting of 18 peptide planes (19 amino acids) with uniform torsion angles of $(\varphi, \psi) = (-65°, -40°)$ except at the 10th residue (between planes 9 and 10), where torsion angles $(\varphi, \psi) = (-85°, -5°)$ were used. A "Canonically curved" helix consisting of 18 peptide planes was built by assigning differing torsion angles for the "hydrophobic" $(\varphi, \psi) = (-59°, -44°)$ and "hydrophilic" $(\varphi, \psi) = (-66°, -41°)$ faces of the helix [13,14]. Lastly, a β-strand was built containing both a twist and a curvature, consisting of eight peptide planes. For all structures the mean secondary structure axis was arbitrarily oriented at $(\Theta, \Phi) = (20°, 60°)$ with respect to the alignment tensor, with the phase of the first peptide plane normal vector $\rho_1^n = 90°$. Residual dipolar couplings were then generated directly from the inter-nuclear vector orientations for the spin pairs HN, $C_\alpha C$, NC′, and $C_\alpha H_\alpha$, using $D_a^{\mathrm{HN}} = -15$, and $R = 1/3$.

4. Results

4.1. Kinked α-helix

The alignment fit to the ${}^1D_{NH}$, ${}^1D_{C\alpha C'}$, ${}^1D_{NC'}$, and ${}^1D_{C\alpha H\alpha}$ data for the kinked helix yielded $(\Theta, \Phi) = (20°, 58°)$, a phase $\rho_1^n = 95°$, and uniform tilt and pitch angles of $\bar{\delta}^n = 104°$ and $\bar{\gamma}^n = -11°$. The RMS deviations of the alignment fit were $\sigma^{\mathrm{NH}} = 4.1$ Hz, $\sigma^{\mathrm{C}\alpha\mathrm{C}'} = 1.4$ Hz, $\sigma^{\mathrm{NC}'} = 0.6$ Hz, and $\sigma^{\mathrm{C}\alpha\mathrm{H}\alpha} = 12.9$ Hz. These RMSD values indicate that the helix possesses significant deviations from an ideal straight helix structure aligned at the $(\Theta, \Phi) = (20°, 58°)$. It is important to note that without knowing the structure before hand, this helix cannot be regarded as "simply" two straight helices connected at a pivot point. Instead, it is a helix with substantial local deviations in peptide plane orientations with respect to the mean helix axis (see Fig. 6).

The alignment parameters were used in the subsequent individual peptide plane fitting to determine the local structure. The standard deviations between target and fit in-plane RDCs were $<10^{-3}$ Hz for all peptide planes. The combination of peptide plane orientations yielding the smallest errors in tetrahedral angles and

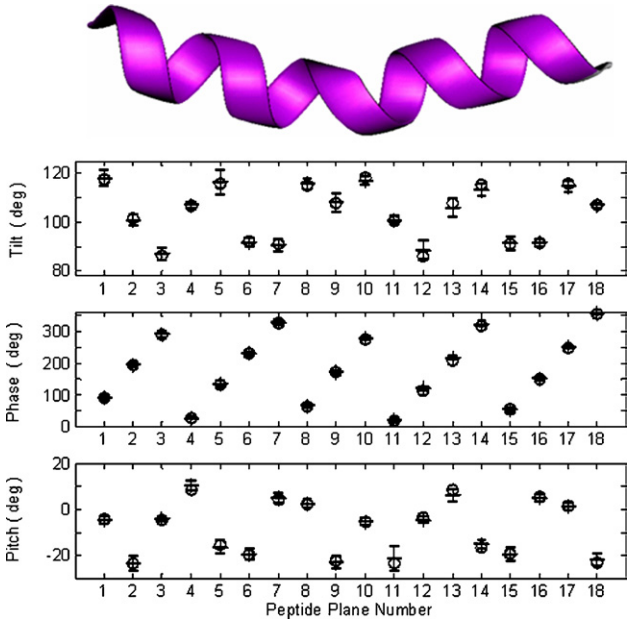

Fig. 6. The structure of the kinked α-helix, shown in a cartoon diagram on top, is represented in the peptide plane coordinate system. The tilt, phase, and pitch angles for the kinked α-helix structure (o) are shown together with the fit peptide plane angle (+). The fit (+) represents the mean fit angle and the error bars the angular RMSD obtained from a Monte-Carlo simulation fitting the RDC data generated from the coordinates with superimposed normally distributed noise.

RDCs gave 0.27° and 0.31 Hz for $T_{\mathrm{NC}\alpha\mathrm{C}'}$ and ${}^{1}D_{H_{\alpha}C\alpha}$ RMSDs, respectively. These small errors are due to variations in the tetrahedral geometry of the model. This best combination of peptide plane orientations gave tilt, phase, and pitch angles which agreed very well with the original structure, yielding angular RMSDs of 0.08°, 0.35°, and 0.11°, respectively (fit not shown). These results demonstrate that individual peptide plane orientations can be very well fit, even when these vary significantly, together yielding a globally kinked helix.

A Monte-Carlo simulation was run by adding random error to the RDCs (see Section 3) to estimate the sensitivity of the fit plane orientations to random measurement errors. The resultant mean fit peptide plane tilt, phase and pitch (+), and the standard deviations are shown together with the corresponding original structure angles (o) in Fig. 6. The figure clearly shows the overall robustness of the procedure. The RMSDs (all peptide planes taken together) are 2.7° for the tilt, 6.6° for the phase, and 2.5° for the pitch. The individual peptide planes 5 and 11 show relatively large errors in tilt and pitch, respectively. This is because at these particular angles in the alignment tensor system the RDC is relatively insensitive to variation of the plane (bond vector) orientation.

4.2. Curved α-helix

The alignment fit to the synthesized RDCs from the curved helix yielded an orientation of $(\Theta,\Phi) = (18°, 73°)$, and phase $\rho_1^n = 74°$, with uniform tilt and pitch angles of $\bar{\delta}^n = 103°$ and $\bar{\gamma}^n = -9°$, respectively. The standard deviations of the fit were $\sigma^{\mathrm{NH}} = 5.5$ Hz, $\sigma^{\mathrm{C}\alpha\mathrm{C}'} = 1.2$ Hz, $\sigma^{\mathrm{NC}'} = 0.5$ Hz, and $\sigma^{\mathrm{C}\alpha\mathrm{H}\alpha} = 10.8$ Hz. As was the case in the kinked helix, these deviations are indicative of local deviations in the structure (non-uniform peptide plane orientations) with respect to the alignment fit axis.

The alignment parameters were used in the subsequent individual peptide plane fitting, yielding RMS deviations between target and fit in-plane RDCs $< 10^{-3}$ Hz for all planes. The combination of peptide plane orientation solutions yielding the smallest errors in tetrahedral angles and RDCs gave 0.33° and 0.20 Hz for $T_{\mathrm{NC}\alpha\mathrm{C}'}$ and ${}^{1}D_{H\alpha C\alpha}$ RMSDs, respectively. This best combination of peptide planes did indeed reproduce the original structure accurately, as evidenced by the fit tilt, phase, and pitch angles RMSDs of 0.07°, 0.22°, and 0.10°, respectively (fit not shown).

Addition of noise to the target RDCs though a Monte-Carlo simulation yielded similar results to those of the kinked helix, and are shown in Fig. 7. The RMSDs were 3.4° for the tilt, 6.3° for the phase, and 2.3° for the pitch. However, for the curved helix the range of tilt angles is significantly smaller, and therefore shows larger relative errors, in particular in the tilt angles of plane 5, 10, and 12. Furthermore, the superimposed error is significant enough to yield two distinct orientations for plane 2. This is manifest in the reasonably large tilt error at this plane, whose mean value differs significantly from that of the original structure.

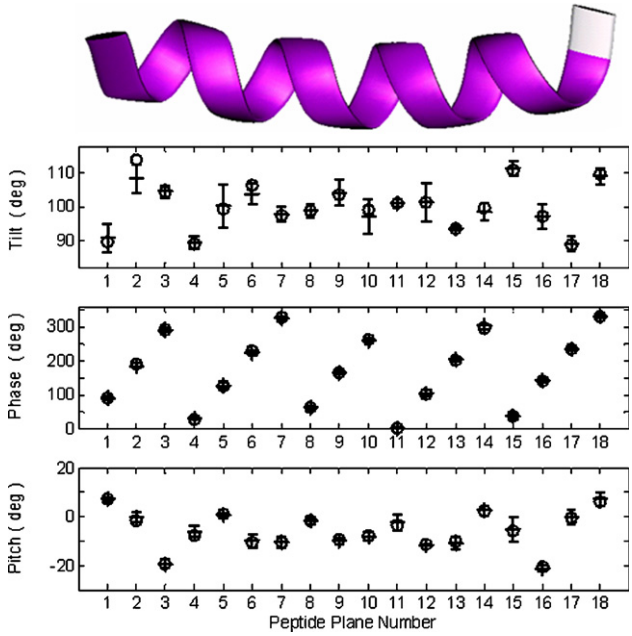

Fig. 7. The structure of the curved α-helix, shown in a cartoon diagram on top, is represented in the peptide plane coordinate system below. The tilt, phase, and pitch angles for the curved α-helix structure (o) are shown together with the fit peptide plane angle (+). The fit (+) represents the mean fit angle and the error bar the angular RMSD obtained from a Monte-Carlo simulation fitting the RDC data generated from the coordinates with superimposed normally distributed noise.

4.3. Irregular β-strand

The alignment fit of the RDCs yielded an orientation of $(\Theta,\Phi) = (22°, 60°)$, and phase $\rho_1^n = 82°$, with uniform tilt and pitch angles of $\bar{\delta}^n = 116°$ and $\bar{\gamma}^n = -72°$, respectively. The fit period was $T = 1.79$ residues/turn. The standard deviations of the alignment fit were $\sigma^{\mathrm{NH}} = 3.1$ Hz, $\sigma^{\mathrm{C}\alpha\mathrm{C}'} = 0.9$ Hz, $\sigma^{\mathrm{NC}'} = 0.5$ Hz, and $\sigma^{\mathrm{C}\alpha\mathrm{H}\alpha} = 5.9$ Hz.

The alignment parameters were used in the subsequent individual peptide plane fitting, which gave standard deviations between target and fit in-plane RDCs $< 10^{-3}$ Hz for all planes. The best-fit combination of peptide plane orientations yielded a standard deviation in tetrahedral angle $T_{\mathrm{NC}\alpha\mathrm{C}'}$ of 0.21° and a standard deviation in ${}^{1}D_{H\alpha C\alpha}$ of 0.76 Hz. The fit tilt, phase and pitch angles agreed very well with the original structure, yielding angular RMSDs of 0.11°, 0.33°, and 0.03°, respectively (fit angles not shown).

Monte-Carlo simulation was again used to generate error estimates for the plane orientation angles. The resultant RMSDs were 2.7° for the tilt, 4.5° for the

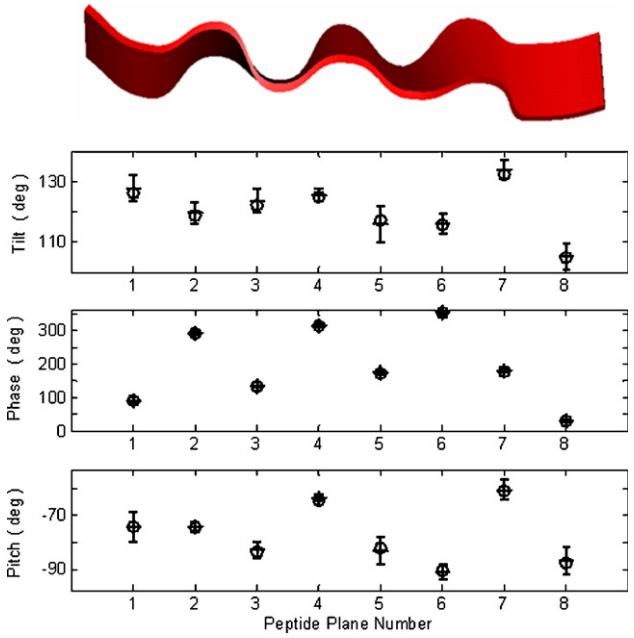

Fig. 8. The structure of the irregular β-strand, shown in a cartoon on top, is represented in the peptide plane coordinate system below. The tilt, phase and pitch angles for an irregular β-strand structure (o) are shown together with the fit peptide plane angles (+). The fit (+) represents the mean fit angle and the error bar the angular RMSD obtained from a Monte-Carlo simulation fitting the RDC data generated from the coordinates with superimposed normally distributed noise. The nature of the β-strand is clearly evident in the phase, which increments by approximately 180° from one peptide plane to the next (mod 2π). The overall upward trend of the phase indicates the larger phase increment (smaller mean period, $T = 1.79$ planes (residues)/turn) than the 180° phase increments of an ideal β-strand.

phase, and 2.2° for the pitch. Fig. 8 shows the peptide plane orientation angles obtained from the Monte-Carlo simulation, demonstrating that the applicability of the procedure is not limited to α-helices.

5. Discussion

The work presented here introduces the general concept of the RDC periodicity planarity correlation that is applicable to not only peptide planes arranged in repetitive and periodical patterns, but also to nucleic acid single stranded helices and duplexes where the planar motifs are nucleic bases, even though the detailed discussion and description have been focused on peptide cases. The geometric constraints of the secondary structure are naturally built into the expressions for the RDCs by the use of coordinate systems which lend themselves to this purpose. Eq. (2) was derived using the spherical coordinated system (see Eq. (1)) with the periodicity isolated in the variable ρ_i (Eq. (2)). In Eq. (4), the custom coordinate system used (see Eq. (3)) contains the periodicity of the peptide plane isolated in the variable γ^n, which is nested within the secondary structure periodicity of the peptide plane normal vector, described by ρ^n. A final coordinate system allows the relationship between neighboring peptide planes and the tetrahedral inter-nuclear vectors to be established (Eqs. (5), (6a), and (6b)). Fundamental to the entire method is the assumption of planarity (Eq. (3)) and the consequent relationship between peptide planes and tetrahedral center (Eqs. (5), (6a), and (6b)). Only the subset of solutions to the RDC data which satisfy these geometric constraints are found. Therefore, the protein secondary structure determined in this manner is the best-fit to the RDC data which consists of peptide planes linked by tetrahedral centers.

The current RDC periodicity–planarity method differs in a further fundamental manner from the direct refinement methods using RDCs: it uses a minimal data size to solve for both the global and the detailed local structure. Instead of relying on a multitude of semi-qualitative distance constraints [15] and dihedral constraints [16] to determine the global and local protein structure before the RDC restraints can be applied for refinement [4], the RDC periodicity–planarity approach determines both global structure and local peptide plane orientations using only the RDC data from the peptide planes and the intervening tetrahedral centers. The plane orientations relative to the alignment tensor determined in this way fully determine the protein backbone secondary structure.

The limited number of measurable RDCs per peptide plane directly implies that the RDCs must be accurately measured to apply the RDC periodicity–planarity method. In particular, it is clear from the basic RDC equation (Eq. (7)) that the accuracy of angular information derived from a particular type of spin-pair depends on the ratio of the RDC random measurement error to the D_a^{AB} of the spin-pair in question. Spin pairs with:

$$D_{AB}/D_a^{AB} = 3\cos^2\theta - 1 + \frac{3}{2}R\cos 2\phi\sin^2\theta, \qquad D_a^{AB} \approx \gamma_A\gamma_B/r_{AB}^3, \tag{7}$$

smaller gyromagnetic moments, or separated by larger distances, yield greater angular error than do spin-pairs with higher gyromagnetic moments, or separated by smaller distances, if the random measurement errors are equal for both. Since all RDCs from a given peptide plane are utilized together in the context of Eq. (4) all RDCs must be measured accurately for that particular plane orientation to be determined accurately. Furthermore, since the in-plane RDCs do not in general uniquely determine tilt, phase, and pitch of a peptide plane, discrimination of the correct plane orientation among the discrete set of possible solutions (see Section 3) is dependent on RDCs of the neighboring tetrahedral centers. Therefore, errors in these must also be considered: depending upon the size of the error on the tetrahedral center RDC and its orientation in the alignment

frame, more than one possible peptide plane orientations may be possible (see below).

Monte-Carlo analysis indicates that realistic simulated random experimental error superimposed on the RDCs does not generally yielding spurious solutions to the peptide plane orientations. The superimposed RDC error in the Monte-Carlo simulations yielded distributions in the tilt, phase, and pitch angles which represent the solution to Eq. (4), with the solutions of neighboring planes' orientation required to be consistent with the RDC of the intervening tetrahedral center. Fig. 9 shows the effect of superimposed simulated random RDC error on the fit tilt, phase, and pitch angles obtained for the canonically curved α-helix (Fig. 7). Fig. 9A shows a typical distribution, with a relatively more accurately defined pitch angle than tilt or phase. The accuracy of the determined peptide plane orientation is dependent upon its orientation in the alignment frame, and some of the planes therefore yielded more sharp distributions, as can be seen for plane 4 (Fig. 9B) of the canonically curved α-helix. However, in some cases the plane and neighboring tetrahedral RDCs yield two equally possible orientation solutions when random noise is superimposed on them. In the Monte-Carlo simulation, this is evidenced by two distinct or semi-distinct (partially overlapping) distributions for the orientation of the peptide plane. Overlapping distributions can lead to a relatively larger error in the plane orientation, or in the case of distinct distributions, to two distinct possible plane orientations. For example, Fig. 9C shows plane 2 of the "canonically curved" α-helix representing a worst-case scenario, with two separate solutions, the incorrect one possessing a tilt angle centered at ~105° and being the predominant population, and the correct peptide plane orientation with tilt angle of ~115° the smaller population. Because the incorrect solution is predominant (statistically most likely), it leads to the error in the Monte-Carlo determined tilt orientation for plane 2 observed in Fig. 7. In cases such as this, where the amount of data does not suffice to unambiguously discriminate between two alternate plane orientations, a second set of RDC data in a second alignment medium should resolve the ambiguity.

The fundamental advance represented by the RDC periodicity–planarity method is due to the ability to directly determine the orientations of all peptide planes in secondary structures with respect to a common reference frame: the alignment tensor. This was made possible by using the known periodicity of secondary structure types and the known periodicity of bond vectors in the peptide planes. Together with the relationship of the peptide planes to the tetrahedral centers, enough constraints exist on the system to define the peptide plane orientations directly with respect to the alignment tensor coordinates. Only the global degeneracy of four possible secondary structure alignments remains. The detailed local structures which yield kinks, curvature, or twists of α-helices and β-strands are in almost all cases unambiguously resolved. This result is in stark contrast to previous interpretation of RDCs, in which the possible solutions to the orientation of a bond-vector connecting spin-pairs was not adequately constrained, yielding too many, *incoherent* possible orientations. These orientations often "compete" with one another in direct refinement using RDCs, and can therefore only be used in refinement of an already well characterized structure [4]. In the RDC periodicity–planarity method however enough of the constraints naturally existing in proteins structure are built directly into the interpretation of the RDCs, and hence the RDCs work *coherently* to yield the global and local structure, and can be used directly in determining the structure.

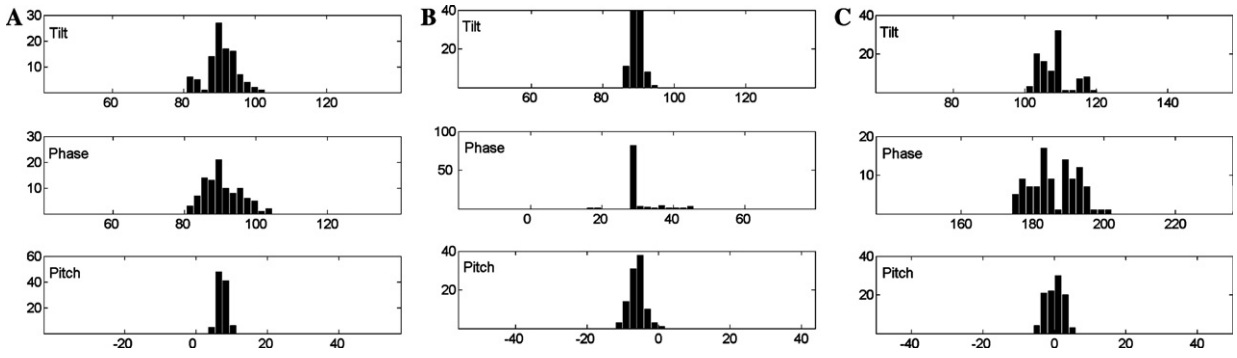

Fig. 9. Types of peptide plane orientation distributions obtained from Monte-Carlo simulation of 100 runs (see Section 3) on the canonically curved α-helix aligned with $(\Theta, \Phi) = (20°, 60°)$. The number of counts per 2° bin is indicated on the vertical axis, with the tilt angle in degrees plotted on top, the phase in the middle and pitch on the bottom. (A) A typical distribution, showing the sharpest distribution in the pitch angle (Plane 1). (B) A sharp distribution indicating a very well-defined peptide plane orientation (Plane 4). (C) A bimodal distribution in the tilt and phase, indicating two alternate peptide plane orientations, which cannot be distinguished on the basis of the single noisy RDC data set. In this particular case, the bimodal distribution in the tilt angle results in the error in the predicted tilt orientation seen in Fig. 7 (Plane 2).

6. Conclusion

The complex periodicity in RDCs was shown to closely reflect the periodicity of secondary structures. The Dipolar wave contains information about both global alignment of protein secondary structure and local peptide plane orientation. By exploiting the known geometric relationships among the atoms in the peptide plane in a periodical secondary structure and their RDCs, we extracted the molecular frame coordinates in the form of peptide plane orientations in relationship to the alignment axis system. These plane orientations were used to determine structures.

6.1. Software availability

Matlab scripts for obtaining alignment, tilt, phase, and pitch angles are available from the authors upon request.

Acknowledgment

We thank Dr. R. Andrew Byrd for encouragement.

References

[1] M.F. Mesleh, G. Veglia, T.M. DeSilva, F.M. Marassi, S.J. Opella, Dipolar waves as NMR maps of protein structure, J. Am. Chem. Soc. 124 (2002) 4206–4207.
[2] J.D. Walsh, J. Cabello-Villegas, Y.-X. Wang, Periodicity in residual dipolar couplings and nucleic acid structures, J. Am. Chem. Soc. 126 (2004) 1938–1939.
[3] A. Mascioni, G. Veglia, Theoretical analysis of residual dipolar coupling patterns in regular secondary structures of proteins, J. Am. Chem. Soc. 125 (2003) 12520–12526.
[4] A. Bax, Weak alignment offers new NMR opportunities to study protein structure and dynamics, Protein Sci. 12 (2003) 1–16.
[5] N. Tjandra, J.G. Omichinski, A.M. Gronenborn, G.M. Clore, A. Bax, Use of dipolar H-1-N-15 and H-1-C-13 couplings in the structure determination of magnetically oriented macromolecules in solution, Nat. Struct. Biol. 4 (1997) 732–738.
[6] H. Zhou, A. Vermeulen, F.M. Jucker, A. Pardi, Incorporating residual dipolar couplings into the NMR solution structure determination of nucleic acids, Biopolymers 52 (1999) 168–180.
[7] J.A. Losonczi, M. Andrec, M.W.F. Fischer, J.H. Prestegard, Order matrix analysis of residual dipolar couplings using singular value decomposition, J. Magn. Reson. 138 (1999) 334–342.
[8] Z.G. Wu, F. Delaglio, N. Tjandra, V.B. Zhurkin, A. Bax, Overall structure and sugar dynamics of a DNA dodecamer from homo and heteronuclear dipolar couplings and P-31 chemical shift anisotropy, J. Biomol. NMR 26 (2003) 297–315.
[9] J.R. Quine, T.A. Cross, Protein structure in anisotropic environments: Unique structural fold from orientational constraints, Concepts Magn. Reson. 12 (2000) 71–82.
[10] R.R. Ketchem, W. Hu, T.A. Cross, High-resolution conformation of gramicidin A in a lipid bilayer by solid-state NMR, Science 261 (1993) 1457–1460.
[11] R. Tycko, P.L. Stewart, S.J. Opella, Peptide plane orientations determined by fundamental and overtone N-14 Nmr, J. Am. Chem. Soc. 108 (1986) 5419–5425.
[12] P. Kuhn, M. Knapp, S.M. Soltis, G. Ganshaw, M. Thoene, R. Bott, The 0.78 angstrom structure of a serine protease: *Bacillus lentus* subtilisin, Biochemistry 37 (1998) 13446–13452.
[13] N. Zhou, B. Zhu, B. Sykes, R. Hodges, Relationship between amide proton chemical-shifts and hydrogen-bonding in amphipathic alpha-helical peptides, J. Am. Chem. Soc. 114 (1992) 4320–4326.
[14] M.F. Mesleh, S.J. Opella, Dipolar waves as NMR maps of helices in proteins, J. Magn. Reson. 163 (2003) 288–299.
[15] K. Wüthrich, NMR of Proteins and Nucleic Acids, Wiley, New York, 1986.
[16] S. Spera, A. Bax, Empirical correlation between protein backbone conformation and C-Alpha and C-Beta C-13 nuclear-magnetic-resonance chemical-shifts, J. Am. Chem. Soc. 113 (1991) 5490–5492.